

# Observation of Weak-Limit Quasiparticle Scattering via Broadband Microwave Spectroscopy of a $d$ -Wave Superconductor

P. J. Turner, R. Harris, Saeid Kamal, M. E. Hayden,\* D. M. Broun, D. C. Morgan, A. Hosseini, P. Dosanjh, G. Mullins, J. S. Preston,<sup>†</sup> Ruixing Liang, D. A. Bonn, and W. N. Hardy  
*Department of Physics and Astronomy, University of British Columbia, Vancouver, B.C., Canada V6T 1Z1*  
 (Dated: October 23, 2018)

There has long been a discrepancy between microwave conductivity measurements in high temperature superconductors and the conductivity spectrum expected in the simplest models for impurity scattering in a  $d$ -wave superconductor. Here we present a new type of broadband measurement of microwave surface resistance that finally shows some of the spectral features expected for a  $d_{x^2-y^2}$  pairing state. Cusp-shaped conductivity spectra, consistent with weak impurity scattering of nodal quasiparticles, were obtained in the 0.6-21 GHz frequency range in highly ordered crystals of  $\text{YBa}_2\text{Cu}_3\text{O}_{6.50}$  and  $\text{YBa}_2\text{Cu}_3\text{O}_{6.99}$ .

PACS numbers: 74.25.Nf, 74.72.Bk

It is now widely accepted that cuprates exhibiting high temperature superconductivity involve a pairing state with  $d_{x^2-y^2}$  symmetry [1]. However, there is considerable debate over the extent to which conventional Bardeen-Cooper-Schrieffer theory can account for the properties of this superconducting state, a debate that is closely related to the difficulty in understanding the peculiar metallic state in these materials. The question is, despite the new physics being encountered in the cuprate phase diagram, is the  $d_{x^2-y^2}$  superconducting state simple? In this letter we present the first low frequency conductivity spectra that answer this in the affirmative, showing an evolution at low temperatures towards the cusp-shaped spectrum expected for weak-limit impurity scattering in a clean  $d$ -wave superconductor. This characteristic spectrum has remained elusive because it only appears at temperatures far below  $T_c$  in very clean crystals, thus necessitating the development of a sensitive bolometric technique for making broadband microwave measurements.

A simple feature of a clean  $d_{x^2-y^2}$  superconductor is that the low energy density of states is expected to have the form  $N(\varepsilon) \propto \varepsilon/\Delta_0$  where the linear energy dependence comes from the linear dispersion of the superconducting gap near its nodes in momentum-space and  $\Delta_0$  is the energy scale of the superconducting gap. At sufficiently low temperatures the microwave conductivity should be governed by the quasiparticle excitations near the nodes. The microscopic details of the scattering mechanism and the framework for calculating the conductivity provide an opening where one might find novel physics entering into the problem. In the low temperature limit, the conventional framework for calculating the conductivity in the superconducting state is a self-consistent  $t$ -matrix approximation (SCTMA) developed to account for impurity pair-breaking effects which modify both  $N(\varepsilon)$  and the electron self-energy [2, 3]. This work showed that the expression for the microwave conductivity for any scatter-

ing strength takes a simple energy-averaged Drude form  $\sigma(\omega, T) = ne^2/m^* \langle [i\omega + \tau^{-1}(\varepsilon)]^{-1} \rangle_\varepsilon$ , where the energy dependence of the scattering rate  $\tau^{-1}(\varepsilon)$  is determined by the strength of the scattering and  $\langle \dots \rangle_\varepsilon$  denotes a thermal average weighted by  $N(\varepsilon)$  [2]. At low  $T$ , the unitary (strong-scattering) limit result has  $\tau^{-1}(\varepsilon) \approx \Gamma_u/\varepsilon$  while the Born limit has  $\tau^{-1}(\varepsilon) \approx \Gamma_B\varepsilon$  (to within logarithmic corrections), where the scale factors  $\Gamma_u$  and  $\Gamma_B$  are determined by the density of impurities. The puzzling failure of this theory has been that neither form resembles the energy-independent  $\tau^{-1}$  inferred from the microwave measurements on  $\text{YBa}_2\text{Cu}_3\text{O}_{6.99}$  by Hosseini *et al.* [4].

Two major technical steps have now led to the discovery of a low temperature regime where some of the expectations of the simple theory seem to hold. First, the samples used in the experiment reported here are of exceptionally high crystalline perfection. Most cuprate materials retain a substantial level of intrinsic disorder due to cation cross-substitution, but the  $\text{YBa}_2\text{Cu}_3\text{O}_{6+x}$  system has a chemical stability that guarantees an extremely low level of cation disorder ( $<10^{-4}$ ). Large improvements in the purity of  $\text{YBa}_2\text{Cu}_3\text{O}_{6+x}$  crystals were brought about by the advent of  $\text{BaZrO}_3$  crucibles, which do not corrode during crystal growth [5]. With a very high degree of atomic order in the  $\text{CuO}_2$  planes, the secondary disorder effect of the off-plane oxygen atoms becomes important. Since intercalation of oxygen into the  $\text{CuO}$  chains in this material (which run along the crystal  $\hat{b}$ -axis) act as the reservoir for hole doping, probing the phase diagram typically involves nonstoichiometry and off-plane disorder. However, a few highly ordered phases are available in this system. Here we concentrate on fully-doped  $\text{YBa}_2\text{Cu}_3\text{O}_7$ , with every  $\text{CuO}$  chain filled, and ortho-II ordered  $\text{YBa}_2\text{Cu}_3\text{O}_{6.50}$ , with every other  $\text{CuO}$  chain filled. The perfection of the fully-doped samples is limited by not being able to anneal to completely full chains,  $\text{O}_{6.99}$  being our limit. The crystalline perfection of the  $\text{YBa}_2\text{Cu}_3\text{O}_{6.50}$  crystals comes from the high purity which in turn allows the development of very long

correlation lengths of the ortho-II order in the 3 crystallographic directions ( $\xi_a=148$  Å,  $\xi_b=430$  Å, and  $\xi_c=58$  Å) [6]. The measurements shown here were performed on mechanically detwinned single crystals of 99.995% purity with dimensions  $(a \times b \times c) \sim (1 \times 1 \times 0.010)$  mm<sup>3</sup>.

The second key step to the results presented here is a measurement technique based on a bolometric method of detection, which provides a natural way of covering the microwave spectrum in more detail than is possible with a set of fixed-frequency experiments. The technique has recently proven useful for measuring resonant absorption in the cuprates [7]. For the present work we have improved the sensitivity of the technique to the pW level necessary for resolving the intrinsic power absorption of a small single crystal, while at the same time employing an in-situ Ag:Au alloy reference sample of known surface resistance that calibrates the absorption absolutely. This is particularly important because it allows compensation for the strong frequency dependence of the microwave field amplitude caused by standing waves in the microwave circuit.

In our system, the microwave surface resistance  $R_s(\omega, T)$  is inferred from the synchronous measurement of the sample temperature rise as the amplitude of the microwave magnetic field  $\vec{H}_{rf}$  is modulated at low frequency (1 Hz). The high- $T_c$  and reference samples are placed in symmetric positions in a rectangular shaped coaxial transmission line with a broadened center conductor designed to ensure spatial magnetic field homogeneity, as depicted in the inset of Fig. 1. The coaxial line is terminated with a short, providing a region where the samples experience predominantly magnetic fields. Both samples are mounted on thin sapphire plates with a small amount of silicone grease. Chip heaters mounted on the thermal stages allow precise calibration of the thermal sensitivity, while the use of a second Ag:Au sample in place of the high- $T_c$  sample confirms the absolute value and frequency independence of the calibration. All measurements use the low demagnetization factor geometry for a thin platelet, with  $\vec{H}_{rf} \parallel \hat{b}$ . Thus the screening currents run along the crystal's  $\hat{a}$ -axis, completing the loop with a short section of  $\hat{c}$ -axis current which we do not attempt to correct for but know to be a small contribution.

Figure 1 shows the frequency dependence of  $R_s$  for  $\hat{a}$ -axis currents in a crystal of  $\text{YBa}_2\text{Cu}_3\text{O}_{6.50}$ . The measurements span 0.6-21 GHz, limited at low frequency where the small dissipation of the sample approaches the resolution limit of the experiment. The 1 GHz values for the rms uncertainty in  $R_s$ ,  $\delta R_s$ , are about 0.2, 0.4, 0.6, and 1.3  $\mu\Omega$  for  $T = 1.3, 2.7, 4.3$ , and 6.7 K respectfully. For the worst case of 6.7 K this translates to  $\delta\sigma_1/\sigma_1 = 0.14$  with uncertainties decreasing correspondingly at higher frequencies and lower temperatures. For clarity, error bars are omitted from the figures. At high frequencies, the apparatus is limited by deviations from the TEM field configuration in the sample region. An overall 5% uncer-

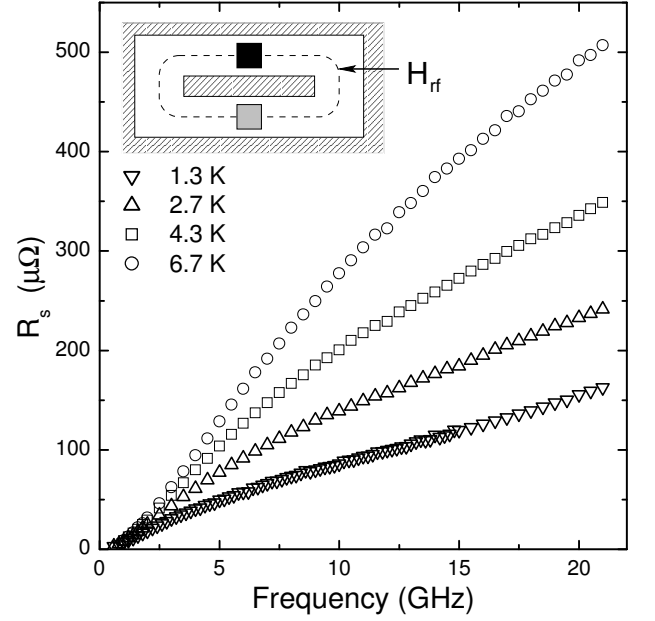


FIG. 1: Low temperature surface resistance data for the  $\hat{a}$ -axis direction of ortho-II ordered  $\text{YBa}_2\text{Cu}_3\text{O}_{6.50}$  obtained from synchronous power absorption measurements. The microwave transmission line used for the measurements is shown in the inset, with the platelet-shaped high  $T_c$  (black) and Ag:Au alloy reference (grey) samples positioned in the regions of homogeneous  $\vec{H}_{rf}$ .

tainty in  $R_s$  is set mainly by the Ag:Au reference-alloy DC resistivity measurement.

In the limit of local electrodynamics, the relevant limit in our sample geometry [8], the surface impedance  $Z_s = R_s + iX_s$  is connected to the complex conductivity  $\sigma = \sigma_1 - i\sigma_2$  via  $Z_s = \sqrt{i\mu_0\omega/\sigma}$ . Measurements of both  $R_s$  and  $X_s$  can be used to determine  $\sigma_1$  and  $\sigma_2$ , but broadband measurements of only  $R_s$  present a problem. A common solution, used in infrared measurements, is to measure a single quantity such as reflectance over a wide enough range that Kramers-Kronig and Fresnel equations can be used to calculate  $\sigma_1$  and  $\sigma_2$ . Another solution is to fit spectra to a model of  $\sigma_1$  and  $\sigma_2$  that automatically satisfies the Kramers-Kronig relations. However, low frequency microwave measurements allow another option for extracting  $\sigma_1(\omega, T)$  from  $R_s(\omega, T)$ . Deep in the superconducting state, both  $\sigma_2$  and  $X_s$  are largely controlled by the screening associated with the response of the superfluid. In the low frequency limit  $X_s = \mu_0\omega\lambda$  and  $\sigma_2 = (\mu_0\omega\lambda^2)^{-1}$  where  $\lambda$  is the London penetration depth. So, at low temperatures a broadband measurement of  $R_s(\omega, T)$  together with a measurement of  $\lambda(T)$  at a single frequency is sufficient to extract the conductivity spectrum  $\sigma_1(\omega, T)$ . Using cavity perturbation techniques with a superconducting loop-gap resonator operating at 1.1 GHz [9] we measure  $\Delta X_s(T) = \mu_0\omega\Delta\lambda(T)$ , where  $\Delta\lambda(T) = \lambda(T) - \lambda(T = 1.2 \text{ K})$  is the temperature de-

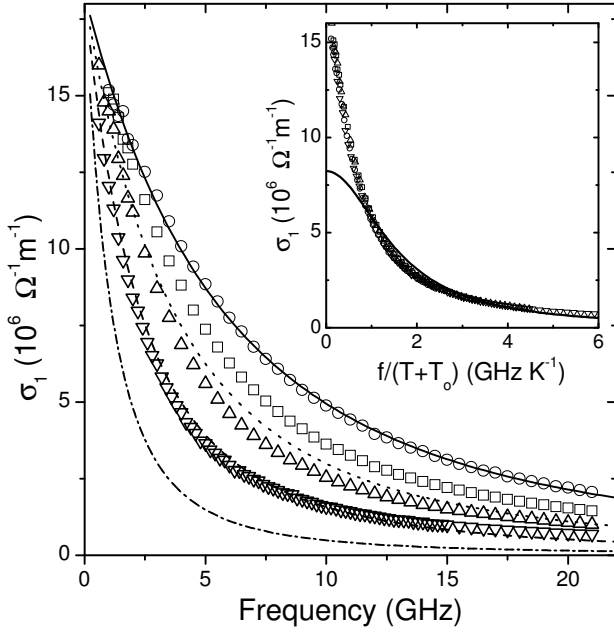


FIG. 2: The low  $T$  evolution of the quasiparticle conductivity spectra of ortho-II  $\text{YBa}_2\text{Cu}_3\text{O}_{6.50}$  (same symbols as Fig. 1). The solid curve is a fit to the 6.7 K data with the Born-scattering model, but the dashed curves show that the model fails to capture the observed  $T$  dependence. The inset shows that the data obey an unusual frequency-temperature scaling  $\sigma_1(\omega, T) = \sigma_1(\omega/[T + T_0])$  with  $T_0 = 2.0$  K. The Drude fit in the inset illustrates the inadequacy of the Lorentzian lineshape.

pendent increase of the London penetration depth from its low temperature limit. Since these measurements do not determine  $\lambda$  absolutely we take the  $T \rightarrow 0$  value to be  $\lambda_0 = 1600$  Å for overdoped  $\text{YBa}_2\text{Cu}_3\text{O}_{6.99}$  as measured by infrared reflectance [10] and  $\lambda_0 = 2600$  Å for underdoped  $\text{YBa}_2\text{Cu}_3\text{O}_{6.50}$ , consistent with  $\mu\text{SR}$  measurements [11]. A more accurate extraction of  $\sigma_1(\omega, T)$  involves a correction for screening by the normal fluid conductivity. To do this we use a self-consistent method that includes contributions to  $\sigma_2(\omega, T)$  both from the superfluid and from the screening component due to quasiparticles [4]. At the low temperatures of this experiment, where there are few quasiparticles to contribute to the screening, this is a small correction having a maximum effect of 8% on  $\sigma_1$  for our highest temperatures and frequencies.

Figure 2 depicts the real part of the quasiparticle conductivity extracted from the broadband  $R_s$  measurements. The strong frequency dependence over intervals as small as 1 GHz (equivalent to a temperature of 0.05 K) shows that the timescale associated with the scattering of low-energy quasiparticles in these extremely clean samples falls within the bandwidth of our measurement. The cusp-like shape of  $\sigma_1(\omega, T)$ , the approximately  $T$ -independent low frequency limit and a tail that falls more

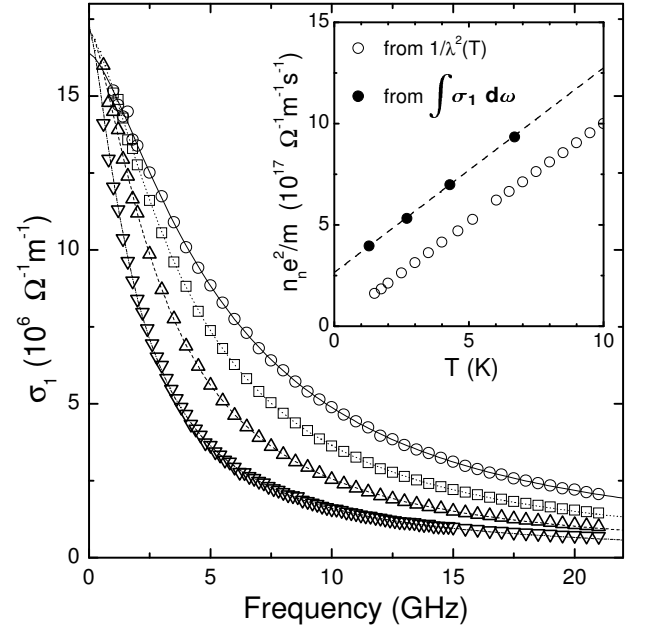


FIG. 3: Phenomenological fits with Eq. 1 (same symbols as Fig. 1). The inset compares the normal fluid density  $n_n e^2/m^*$  obtained by integrating Eqn. 1 with the loss of superfluid density inferred from 1.1 GHz  $\Delta\lambda(T)$  data. The dashed line has the slope of the open symbols, and the agreement indicates that the normal-fluid and superfluid spectral weight obey the conductivity sum rule, although a residual normal fluid term is implied.

slowly than  $1/\omega^2$  are all features expected for Born scattering. The solid curve in Fig. 2 shows a convincing fit to the 6.7 K data using the energy-averaged Drude form with  $\tau^{-1}(\varepsilon) = \Gamma_B \varepsilon$ , indicating that the overall shape of the spectrum is well-described by the weak scattering calculation with fit parameters  $\hbar\Gamma_B = 0.032$  and  $ne^2\hbar/(m^*\Delta_0) = 5.9 \times 10^5 \Omega^{-1}\text{m}^{-1}$ . The other curves in Fig. 2 are the Born-limit predictions for the lower temperatures, using the parameters that fit the 6.7 K data. It is clear that this model progressively underestimates the spectral weight as  $T$  is reduced, and because of this a global fit for all temperatures produces results that are less satisfactory. The inset of Fig. 2 shows that the  $\sigma_1(\omega, T)$  data scale as  $\omega/(T + T_0)$  with  $T_0 = 2.0$  K, rather than scaling as  $\omega/T$  as expected in the Born limit. Hence, the weak scattering limit captures the frequency dependence of the data, but the requirement of the SCTMA model that the spectral weight vanish as  $T \rightarrow 0$  leads to disagreement.

In order to fit to the spectra, we adopt a phenomenological form for  $\sigma_1(\omega, T)$  that captures the Born-lineshape features, namely the cusp-like shape and high frequency tail:

$$\sigma_1(\omega, T) = \sigma_0 / [1 + (\omega/\Gamma)^y]. \quad (1)$$

We fit directly to  $R_s(\omega, T)$ , thereby automatically ac-

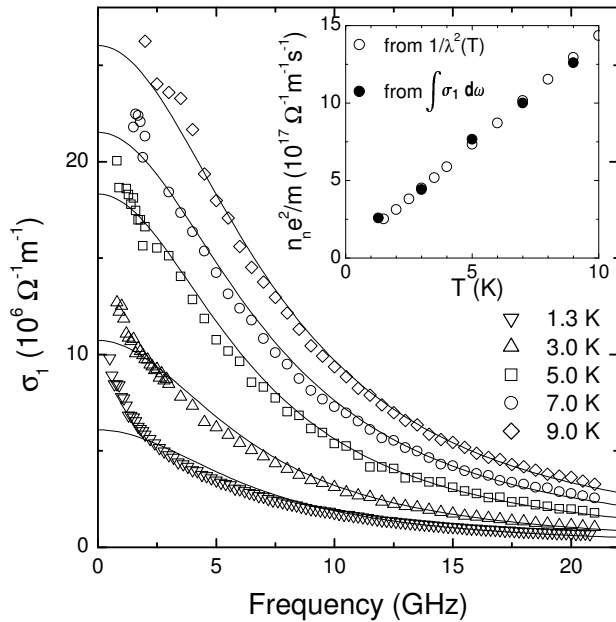


FIG. 4: The conductivity spectrum of a fully-doped sample of  $\text{YBa}_2\text{Cu}_3\text{O}_{6.99}$  in the  $\hat{a}$ -direction. The Drude fits to the spectra highlight the evolution from a cusp-like shape to a more Lorentzian lineshape with increasing temperature.

counting for the quasiparticle screening. Fig. 3 shows the fits to individual spectra using this model where the parameters  $\sigma_o$  and  $y$  remain relatively constant, taking average values of  $1.67(\pm 0.05) \times 10^7 \Omega^{-1}m^{-1}$  and  $1.45(\pm 0.06)$  respectively. The parameter  $\Gamma$  varies approximately linearly in  $T$  with fit values 12.1, 19.2, 26.3, and  $35.0 \times 10^9 \text{sec}^{-1}$ . Although these fits also suggest the unusual frequency-temperature scaling discussed previously, enforcing it in the model reduces the agreement in the spectral weight comparison. The fits can be integrated in order to obtain *absolutely* the temperature dependent spectral weight associated with the normal fluid. In the inset of Fig. 3 this normal fluid spectral weight is compared to the spectral weight lost from the superfluid as determined independently by the measurements of  $\Delta\lambda(T)$ . The slopes agree to within 2%, a good indication that the model is capturing the oscillator strength at higher frequencies. It is important to note that at low  $T$  this comparison is independent of the choice of  $\lambda_0$  to first order since  $\sigma_1 \approx 2R_s/(\mu_0^2\omega^2\lambda_0^3)$  and  $\Delta(1/\lambda^2) \approx -\Delta\lambda/\lambda_0^3$ . The offset apparent in the normal fluid density corresponds to a  $T = 0$  residual normal fluid.

The discovery of a cusp-shaped spectrum for the low temperature conductivity of  $\text{YBa}_2\text{Cu}_3\text{O}_{6.50}$  seems at odds with the Drude fits ( $y = 2$  in Eq. 1) that were found to reasonably describe the spectra inferred from fixed-frequency microwave measurements on fully-doped  $\text{YBa}_2\text{Cu}_3\text{O}_{6.99}$  [4]. To resolve this conflict, broadband conductivity spectra were obtained for the  $\hat{a}$ -axis of a crystal of the fully doped material, shown in Fig. 4. At

the lowest temperatures there is indeed a cusp-like spectrum, similar to the one seen in the underdoped ortho-II sample. The reason this was not seen in earlier measurements is that the spectrum gives way to a more Lorentzian lineshape above 4 K, as indicated by the progressively better fit to a Drude model with increasing temperature; the 5 spectra do not scale in the manner seen for  $\text{YBa}_2\text{Cu}_3\text{O}_{6.50}$ . Hosseini *et al.* concluded that the scattering rate was nearly temperature independent below 20 K at a value of  $\tau^{-1} = 5.6(\pm 0.6) \times 10^{10} \text{sec}^{-1}$ , and here we find  $\tau^{-1} = 4.4(\pm 0.3) \times 10^{10} \text{sec}^{-1}$  with the decrease likely due to continued improvements in the sample purity. The integration of the Drude model captures the oscillator strength rather well, except at the lowest temperatures where the fits are too poor for us to comment upon an extrapolated residual value. It is not yet clear why the non-Lorentzian lineshapes are restricted to such low temperatures in the fully doped sample.

To conclude, we have provided the first highly detailed measurement of the quasiparticle conductivity spectrum in the disorder-dominated regime of an extremely clean  $d$ -wave superconductor. This regime has been accessed by using well-ordered crystals with very high purity, measured with a broadband microwave technique whose frequency range matches the very small quasiparticle scattering rate in the samples. A number of puzzles remain, particularly the residual normal fluid inferred from extrapolations to  $T = 0$ , a phenomenon that is seen to a much greater degree in other cuprates [12, 13]. The cause of the evolution from a cusp-like spectrum to a more Lorentzian lineshape in  $\text{YBa}_2\text{Cu}_3\text{O}_{6.99}$  is also unclear and may require a more sophisticated scattering model that employs intermediate scattering strengths, neither Born nor unitary. Nevertheless, several features of the quasiparticle scattering dynamics are characteristic of Born-limit scattering, namely a cusp-shaped conductivity spectrum seen at low temperatures. Additional physics such as order parameter suppression at impurity sites [14] might be needed to resolve the remaining puzzles, but the data presented here provide a simple starting point that is quite close to the expectation for nodal quasiparticles scattered weakly by impurities.

We gratefully acknowledge useful discussions with A.J. Berlinsky, C. Kallin, and P.J. Hirschfeld, as well as financial support from the Natural Science and Engineering Research Council of Canada and the Canadian Institute for Advanced Research.

\* Permanent address: Dept. of Physics, Simon Fraser University, Burnaby, B.C., Canada, V5A 1S6.

† Permanent address: Dept. of Physics and Astronomy, McMaster University, Hamilton, ON, Canada, L8S 4M1.

[1] C. C. Tsuei and J. R. Kirtley, Rev. Mod. Phys. **72**, 969

- (2000).
- [2] P. J. Hirschfeld, W. O. Putikka, and D. J. Scalapino, Phys. Rev. Lett. **71**, 3705 (1993); Phys. Rev. B **50**, 10250 (1994).
  - [3] C. T. Rieck, D. Straub, and K. Scharnberg, J. Low Temp. Phys. **117**, 1295 (1999).
  - [4] A. Hosseini et al., Phys. Rev. B **60**, 1349 (1999).
  - [5] A. Erb, E. Walker, and R. Flukiger, Physica C **258**, 9 (1996); R. X. Liang, D. A. Bonn, and W. N. Hardy, Physica C **304**, 105 (1998).
  - [6] R. X. Liang, D. A. Bonn, and W. N. Hardy, Physica C **336**, 57 (2000).
  - [7] Y. Matsuda et al., Phys. Rev. B **49**, 4380 (1994); O. K. C. Tsui et al., Phys. Rev. Lett. **73**, 724 (1994); M. Gaifullin et al., Phys. Rev. Lett. **83**, 3928 (1999).
  - [8] I. Kosztin and A. J. Leggett, Phys. Rev. Lett. **79**, 135 (1997).
  - [9] W. N. Hardy et al., Phys. Rev. Lett. **70**, 3999 (1993).
  - [10] D. N. Basov et al., Phys. Rev. Lett. **74**, 598 (1995).
  - [11] R. I. Miller et al. (Unpublished).
  - [12] D. M. Broun et al. (Unpublished).
  - [13] J. Corson et al., Phys. Rev. Lett. **85**, 2569 (2000).
  - [14] M. H. Hettler and P. J. Hirschfeld, Phys. Rev. B **61**, 11313 (2000).